Long-term performance of galvanic anodes for the protection of steel reinforced concrete structures

4 authors, including:

Deepak Kamde
Indian Institute of Technology Madras

23 PUBLICATIONS   35 CITATIONS

SEE PROFILE

Radhakrishna Pillai
Indian Institute of Technology Madras

147 PUBLICATIONS   788 CITATIONS

SEE PROFILE

G. Sergi
Vector Corrosion Technologies Ltd

27 PUBLICATIONS   495 CITATIONS

SEE PROFILE

Some of the authors of this publication are also working on these related projects:

Project   Performance of Fusion-Bonded-Epoxy coated steel embedded in concrete View project

Project   PhD work View project

Journal Pre-proof

Long-term performance of galvanic anodes for the protection of steel reinforced concrete structures

Deepak K. Kamde, Karthikeyan Manickam, Radhakrishna G. Pillai, George Sergi

Manuscript ID: JBE-D-21-02393

Manuscript title: Long-term performance of galvanic anodes for the protection of steel
                   reinforced concrete structures

Authors: Deepak K Kamde, Karthikeyan Manickam, Radhakrishna G. Pillai,
                   and George Sergi

Author Statement

1. **Deepak K. Kamde:** Conceptualization, Methodology, Investigation, Formal Analysis, Visualization, Writing - original draft

2. **Kathikeyan Manickam:** Investigation, Formal analysis, and Writing - Review & Editing

3. **Radhakrishna G. Pillai**: Conceptualization, Writing - Review & Editing, Visualization, and Funding acquisition

4. **George Sergi:** Conceptualization, Writing - Review & Editing, Visualization, and Resources

1 # Long-term performance of galvanic anodes for the protection of steel reinforced concrete structures

3 Deepak K. Kamde‡*, Karthikeyan Manickam*, Radhakrishna G. Pillai*, and George Sergi**

4 ‡deepak.kamde89@gmail.com

5 *Department of Civil Engineering, Indian Institute of Technology Madras, Chennai, India
6 **Vector Corrosion Technologies, Cradley Heath, United Kingdom

7 ## **ABSTRACT**

8 Corrosion is one of the major deterioration mechanisms of reinforced concrete structures. The

9 conventional patch repair without addressing the root cause of the corrosion can lead to

10 repeated repairs. Therefore, a form of cathodic protection (CP) using galvanic anodes is a

11 viable electrochemical technique to mitigate corrosion. However, practitioners hesitate to

12 adopt CP for repair due to the lack of evidence and limited knowledge on the long-term

13 performance of galvanic anodes in concrete systems. For this, two reinforced concrete panels

14 with and without discrete galvanic anodes were cast with admixed chlorides and exposed to a

15 natural environment for 12 years. Electrochemical measurements, such as depolarized

16 corrosion potentials and corrosion rate of the rebars, and output protection current density of

17 the galvanic anodes were measured. In addition, physico-chemical characteristics such as

18 elemental composition, residual lithium content, pH, pore volume, and pore size distribution

19 in the encapsulating mortar were determined on a 12-year in-service galvanic anode. This

20 paper indicates that the alkali-activated galvanic anodes can protect the steel rebars from

21 corrosion for at least 12 years. Analysis after 12 years showed that the pores in encapsulating

22 mortar were partially filled with zinc corrosion products, resulting in substantial pore blockage

23 surrounding the zinc metal. This led to a reduction in the pH buffer in the vicinity of the zinc

24 metal. Also, characteristics of tie wire-zinc metal interface may affect the long-term

25 performance of galvanic anodes. Based on this study, specifications are proposed to help

26 manufacturers to design durable galvanic anode systems.

27 *Keywords: Concrete, steel, chloride, corrosion, repair, galvanic anodes, cathodic protection.*

28 **<u>LIST OF SYMBOLS AND ABBREVIATIONS</u>**

%bwob	:	% by weight of binder
CP	:	Cathodic protection
dcritical	:	Critical pore size
MIP	:	Mercury Intrusion Porosimetry
RC	:	Reinforced concrete
RR	:	Reference region
SCE	:	Saturated calomel reference electrode
EDX		Energy Dispersive X-ray Analysis

29

1 INTRODUCTION

Worldwide, many reinforced concrete (RC) structures were built for a design service life of about 50 years (designed by old standards). Most of them are facing distress due to corrosion of reinforcement. Protection of these structures is utmost important. The emphasis on protection of these structures varies across the globe depending on the period of major economic developments. In addition, many nations in the past two decades have built many RC infrastructure systems such as railways, highways, buildings, and ports for a desired service life of 100 years. Many of them are located in a chloride-rich environment. To achieve such long service life, RC systems (concrete and steel) should have adequate corrosion resistance. However, due to accelerated construction, much of the infrastructure are built without the quest for quality of construction practices and materials, which can result in premature corrosion [1–4]. NACE Impact Report states that about 50% of structures require major repair within ten years after construction [5]. This leads to a huge construction budget to refurbishment and repair of existing structures [6]. Generally, conventional repairs, such as patchwork using complete or partial replacement of concrete/mortars, are adopted to repair RC systems. The patch repairs alone do not address the root cause of corrosion and create the difference in the electrochemical characteristics of steel rebar in parent and repair concrete, leading to premature failure of repair and need for repeated repair. The repeated repairs can be eliminated by the use of cathodic protection (CP) systems using galvanic anodes in the critical locations. Critical locations can be identified by detecting locations where corrosion is already initiated and by estimating residual service life of structural elements where corrosion is not yet initiated, but may initiate within a few years (say, less than 10 years). However, very few structures are provided with CP systems to repair the RC systems. For example, in India, only about 70 structures were repaired using galvanic anodes until 2020 [7]. The practitioners are hesitant to use the galvanic anodes due to (i) the limited availability of evidence of the long-term performance of galvanic anode systems in RC structures, (ii) limited knowledge on corrosion

56 characteristics of galvanic anodes in-service, and (iii) unavailability of standards or guidelines

57 in developing nations to select and use the galvanic anodes, which are the focuses of this paper.

58   The remainder of the paper is organized in the following manner: first, the difference

59 between repair of full structures with and without galvanic anodes is discussed. Then, a

60 literature review on long-term performance and the factors affecting the long-term performance

61 of galvanic anodes is discussed. After that, an experimental program to evaluate the long-term

62 performance of galvanic anodes is discussed. The results from the long-term electrochemical

63 assessment and the effect of physico-chemical characteristics of galvanic anodes on their

64 performance are presented. Based on the results, a list of specifications is proposed to facilitate

65 and ensure the long-term performance of galvanic anodes. Finally, conclusions from this

66 research are presented.

67 **1.1   Repair of reinforced concrete systems**

68 Figure 1 shows the difference in the patch repair without and with galvanic anodes. If patch

69 repair is employed without galvanic anodes (PR strategy), the following consequences can

70 occur (see Figure 1(a)):

71 (i)   **Incipient Anode effect, sometimes referred to as the Halo or Ring effect**:

72   Following repair, the rebar in parent and repair concrete is exposed to different

73   physical (relative humidity, voids, cracks, etc.) and chemical (chloride

74   concentration, pH, etc.) conditions. Prior to repair, steel adjacent to the corroding

75   steel is receiving a level of cathodic protection by the corroding (anodic) region.

76   After repair, this fortuitous local protection is removed so that the above mentioned

77   variation in properties between parent concrete and repair material create an

78   electrochemical potential difference on the rebar surface stretching across the

79   interface of parent and repair concrete [8,9] — leading to the formation of a

80   corrosion cell and accelerated corrosion around the perimeter of the patch repair

81   [9,10].

82   (ii)   **Residual chloride effect**: The rebar in the repaired region, especially if the parent

83   concrete surrounding the steel is not totally removed, may continue corroding due

84   to residual chlorides on the steel rebar surface [7]. This can continue the reduction

85   of the cross-sectional area of rebar even after the repair.

86   (iii)   **Hidden/upcoming corrosion**: This concerns the rebar in the parent concrete which

87   was not addressed at the time of repair either because there was no sign of corrosion

88   or the electrochemical measurements indicated no corrosion activity. However, in

89   a matter of a few months or years; new, and existing chlorides in the concrete will

90   further diffuse into the concrete and initiate the corrosion of steel located in non-

91   patched parts of the structure. This will lead to corrosion of the rebars in locations

92   where repair was not carried out in the earlier intervention.

93   As a result, these repair strategies can fail within about five years [6,7,11]. Soon, a

94 large number of structures may undergo repeated repair — resulting in a large number of

95 accumulation of structures for repair [9,12]. Therefore, there is a dire need to adopt a suitable

96 repair strategy, which can arrest the corrosion due to Incipient Anode effect, sometimes

97 referred to as the Halo or Ring effect, residual chloride effect, and hidden/upcoming corrosion.

98   Figure 1(b) shows how the repair using galvanic anodes can eliminate such effects and

99 help to facilitate a durable repair life [13]. Here, the anode is more electrochemically negative

100 (say −1100 mV) than the steel rebar (say −350 mV). They are electrically connected using tie

101 wires to the rebar and concrete act as the ionic conductor [14]. The potential difference across

102 the galvanic anode and rebar is more than the potential difference between two points on steel

103 rebar at the repaired or parent concrete, or interface of parent and repair concrete [15].

104 Therefore, the metal in galvanic anode preferentially corrodes to protect the rebars up to the

105 throwing distance until the galvanic anode is consumed. The throwing distance is the area or

106 sphere of influence surrounding the galvanic anode up to which it can protect the rebars from

107 corrosion. The throwing power depends on various factors such as type of anode used,

108   resistivity of concrete, rate of corrosion of steels, relative humidity of concrete, etc. [16,17].

109   Therefore, the design of CP systems using galvanic anode (numbers and location) is case-

110   specific and is decided based on throwing power of the galvanic anodes [18].   To address

111   hidden or upcoming corrosion, estimating the residual service life of structural element can

112   help in deciding if the structural element needs immediate attention or can be addressed later.

113   If residual service life is less than 10 years, then installation of galvanic anodes in these

114   locations can delay the initiation of corrosion (see Figure 1(c)).   If repair of structure is

115   adequately planned by installation and replacement of galvanic anodes, it is reported that the

116   level of civil infrastructure needing repair can be decreased by 2 to 5 times [8,19].   The

117   performance of galvanic anodes depends on various factors, which are discussed later in this

118   paper.

(a) Patch repair without anode

(b) Patch repair with galvanic anode

(c) Galvanic anodes for CPrev in the locations where corrosion has not yet initiated
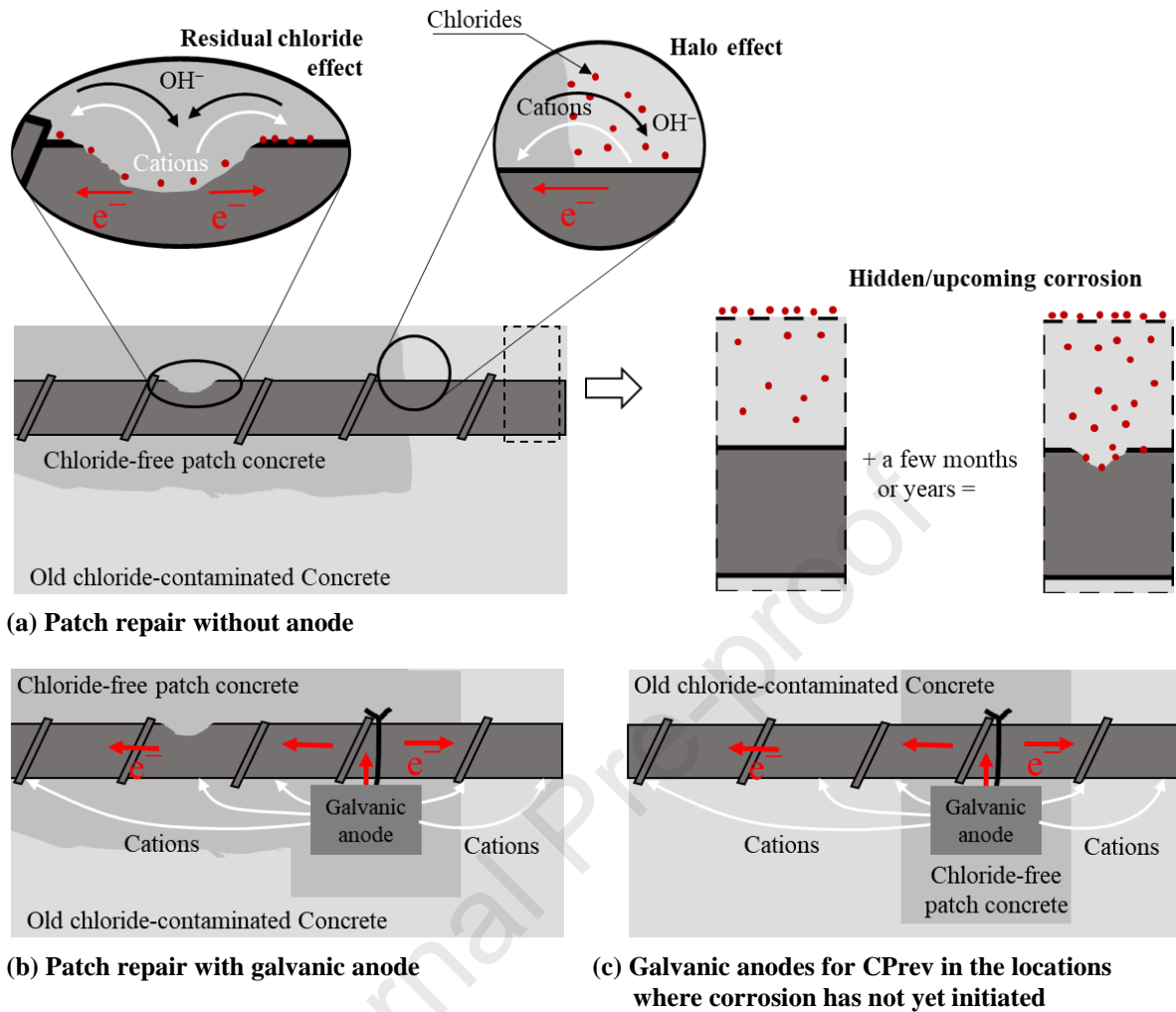
119 **Figure 1: Schematic of the patch repair without and with CP using galvanic anodes**

120 **1.2 Performance assessment of galvanic anodes in reinforced concrete systems**

121 Conventionally, the performance of galvanic anode CP systems in concrete is assessed based

122 on the '100 mV potential shift' of the steel over a period of 24 hours as per ISO EN 12696 [20].

123 For this, the following measurements are required:

124   (i)   **instant-off potential ($E_{i\text{-Off}}$)**: the potential of steel rebars with respect to reference

125   electrode measured within 1 second of disconnecting the anode from the steel rebars

126   (ii)   **24-hour depolarized potential ($E_{24\text{-h}}$)**: the potential of steel rebars with respect to

127   a reference electrode after the anodes are disconnected for 24 hours.

128 As per ISO EN 12696, the difference between $E_{i\text{-Off}}$ and $E_{24\text{-h}}$ should be greater than 100 mV

129 [20]. For this, monitoring box is required to be installed at specific locations on the structures,

130   which is mostly not practiced or not maintained for a long time, which has hindered their long-

131   term performance evaluation [7]. Much of the literature reports that galvanic anode CP systems

132   are primarily designed to offer corrosion prevention, i.e. prevent initiation of corrosion, and

133   cannot achieve 24 h depolarization of 100 mV [21,22]. Therefore, instead of '100 mV

134   potential shift' criterion, the measurement of depolarized potential or the rate of corrosion of

135   the steel in a depolarized state is adopted in this study. This can provide true corrosion

136   conditions of steel rebar surfaces [19].

137   **1.3   Factors affecting the long-term performance of galvanic anodes in concrete**
138   **systems**

139   Figure 2 shows a schematic of typical alkali-activated discrete galvanic anodes with three

140   important elements: (i) galvanic metal, (ii) encapsulating mortar, and (iii) tie wires. The shape

141   and size of anodes vary with manufacuturers and the purpose of use. Galvanic metal corrodes

142   to protect the reinforcement and is selected such that it is more electronegative than steel rebars.

143   Commonly used galvanic metals are magnesium, aluminum, zinc, or their alloys [9]. To keep

144   the galvanic metal active for corrosion, the galvanic metals are embedded in specially

145   formulated encapsulating mortar [8]. The activating agent in the encapsulating mortar,

146   however, should not aggravate the corrosion of steel rebars [23]. Details on the required

147   characteristics of encapsulating mortar are discussed later.

148
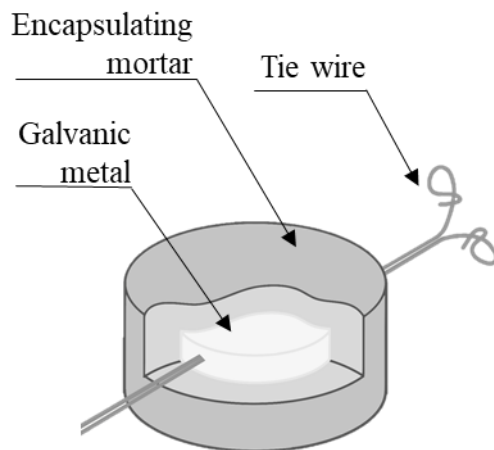
149
150 **Figure 2 Schematic of typical alkali-activated discrete galvanic anode**

151 Many literature worldwide (from Netherlands, England, USA, Canada, India, and Venezuela)

152 report that the good quality galvanic anodes can perform for a service life of 10 to 25 years

153 [7,19,24–26]. The performance of galvanic anodes depends on various factors, such as

154 resistivity of of old and repair concrete, relative humidity of concrete, and steel density to be

155 protected, pH, and porosity of encapsulating mortar, relative humidity at the interface of a

156 galvanic metal and encapsulating mortar. The factors such as steel density, the relative

157 humidity of concrete, and resistivity of concrete are well reported in the literature [15]. Many

158 of these factors can be accommodated by adopting adequate design. However, there are a few

159 factors such as pore volume, pH of encapsulating mortar and effect of alteration of

160 encapsulating mortar characteristics during service, which can influence the performance of

161 galvanic anodes [27,28] are discussed later.

162 *1.3.1   Activators and humectants*

163 The continuous and long-term corrosion of zinc can be achieved by using adequate

164 encapsulating mortar with (i) activators and (ii) humectants [29,30]. Activators increase the

165 dissolution kinetics of anodes and maintain a high corrosive environment around the zinc metal

166 [31] and are classified into two types: (i) halide and (ii) alkali activators [14,32]. Halide

167 activators such as fluoride, chloride, bromide, iodide act as catalysts to maintain a continuous

168   corrosive environment around the anode metal. As the zinc corrodes, the soluble corrosion

169   products migrate through encapsulating mortar, aiding the continuous corrosion of the metal

170   [33]. However, they may lead to corrosion of steel rebars due to the diffusion of the halide

171   anions towards the steel surface, especially when the anodes are placed close to the rebar[23] .

172   On the other hand, alkali activators, such as lithium hydroxide, sodium hydroxide, potassium

173   hydroxide, help in maintaining the pH of the encapsulating mortar to more than 14, thereby,

174   keeping the zinc active [23,34,35]. During this process, these activators get consumed and can

175   lead to the reduction of pH at galvanic metal-encapsulating mortar. For example: zinc oxidises

176   by loosing its two electrons and reacts with an equivalent amount of OH^-, which has to be

177   supplied by the activator, and is a service life determining factor (as is mass of zinc) [see

178   Equations 1 and 3].

179   $$Zn \rightarrow Zn^{2+} + 2e^- \qquad (1)$$
180   $$Zn^{2+} + 4OH^- \rightarrow Zn(OH)_4^{2-} \qquad (2)$$
181   $$Zn(OH)_4^{2-} \rightarrow ZnO + 2OH^- + H_2O \qquad (3)$$

182   Zinc reacts with both acids and bases to form salt. However, the rate of corrosion of zinc is

183   high at pH less than 6 (acidic) and greater than 12.5 (basic) [36]. The rate of corrosion of Zn

184   is relatively low for pH between 6 to 12.5 [27], which can also be termed as passivation of

185   zinc". Therefore, maintaining high alkalinity in encapsulating mortar of alkali-activated mortar

186   is essential. It was reported that the activity of zinc can be enhanced by adding either

187   170 g KOH/100g of zinc or by 73 g LiOH/100g of zinc [8,27]. In another investigation, it was

188   reported that the concentration of LiOH was significantly reduced in the encapsulating mortar

189   after about 14 years of service — leading to a decrease in pH from a designed value of 14.6 to

190   13.8 [19]. However, these anodes were intended to achieve repair life of 10 years, which was

191   designed by providing sufficient zinc and lithium hydroxide content in the encapsulating

192   mortar. This reduction in pH can result in the reduced effectiveness (say, output current,

193   throwing distance, etc.) of the galvanic anode [19], which is why the amount of added alkali to

194   the activating mortar should be determined before production so that the desired service life is

195   achieved.

196   Humectants are hygroscopic materials, which maintain adequate humidity around the

197   anode metal for continuous corrosion of the galvanic metal. They also reduce the build-up of

198   ions at the metal surface to facilitate ionic conduction by allowing them to diffuse (a slow

199   process) into the surrounding moist pore structure [24,29,30]. A few commonly used

200   humectants are lithium bromide, lithium nitrate, calcium chloride, etc. During the process of

201   ionic conduction and electrochemical reactions, the concrete in the vicinity of steel will be

202   enriched with ions such as OH^-, Li^+, Na^+, and K^+. The region around the anode will be enriched

203   with chlorides and other anions due to the diffusion or migration of ions from chloride

204   contaminated concrete [37], and may affect the performance of the galvanic anode.

1.3.2   Characteristics of encapsulating mortar

206   The pore structure of the encapsulating mortar provides space for accommodating the zinc

207   corrosion products and interconnected pores provide the path for movement of zinc corrosion

208   products [8]. It was reported that the pore volume of 16-23% performed best [24,38]. Another

209   research by Schwarz et al. (2016) reported that the encapsulating mortar with volumetric

210   porosity of more than 35% can help to provide a path for movement of zinc corrosion products

211   away from the anode – making fresh zinc surface available for corrosion [27]. Encapsulating

212   mortar with low pore volume can result in clogging of pores with corrosion products and hinder

213   the movement of corrosion products and reduce the ionic transport through the encapsulating

214   mortar [38,39]. Therefore, the pore structure of encapsulating mortar should be designed such

215   that it diffuses the corrosion products away from the zinc metal to make unreacted zinc

216   available for corrosion. The investigation on various pore volume is out of scope of this paper.

217   In addition to pore volume, pH of encapsulating more plays an important role. An advantage

218   of highly alkaline encapsulating mortar (pH>14) is that the zinc corrosion products exist as

219　soluble zincate ions, which can migrate through the pores away from the zinc-mortar interface

220　and maintain clear pathways for current flow for longer period [19]. The authors could not

221　find literature on evaluating the effects of the reduction of porosity of encapsulating mortar on

222　the long-term performance of anodes, which is one of the focuses of this paper.

223　**2　RESEARCH SIGNIFICANCE**

224　As detailed in Section 1.1, conventional patch repairs can result in repeated repairs of adjacent

225　regions. The National Association of Corrosion Engineers IMPACT report states that nearly

226　4% of worldwide GDP is spent to control corrosion of infrastructure [5], most of which is spent

227　to repair the concrete systems. The adequate implementation of CP using galvanic anodes for

228　full structure as CP and CPrev can reduce the frequency of repair and cost of corrosion. The

229　results presented in this paper show that suitable galvanic anodes can protect RC systems for

230　more than 12 years. It is hoped that this will encourage practitioners to incorporate galvanic

231　anodes in the repaired areas of RC systems to significantly prolong their performance. The

232　specifications proposed in this paper can help to design durable galvanic anode systems.

233　**3　EXPERIMENTAL METHODS**

234　The experimental program is designed in two phases, Phase I: long-term performance of

235　galvanic anodes and Phase II: Physico-chemical characterization of a 12-year-old galvanic

236　anode, which is aiming to identify factors affecting the long-term performance of galvanic

237　anodes.

238　**3.1　Phase I: Long-term performance of galvanic anodes**

239　*3.1.1　Specimen preparation and exposure condition*

240　　　　Figure 3(a) shows the schematic of the panels with a dimension of $1 \times 1 \times 0.25$ m. For

241　this, 32 mm diameter rebars were cut to a length of 1.05 m. The rebars were placed 100 mm

242　apart and electrically disconnected to each other (Figure 3(b)). A total of 18 rebars, 9 top and

243　9 bottom rebars, were placed so that the top set of rebars were ≈ 85 mm away from the

244   bottom set. The steel to concrete surface area ratio was 1. For this, only top and bottom surface

245   area of concrete panel were considered. The top face of the panel will augment to the severe

246   exposure condition by ingress of moisture and oxygen to the steel rebars, whereas, bottom face

247   of panel will only be provide the access of oxygen, but not moisture. Side faces were not

248   considered because the extent of ingress of moisture and oxygen from sides will be limited to

249   a few mm from either side face of the panel. Two panels (i) with and (ii) without galvanic

250   anodes were cast. To simulate the condition of existing structures with chlorides in concrete,

251   the concrete in both panels was premixed with 2% chloride by weight of cement (%bwoc).

252   Panel 1 was divided into three parts considering the type of anode installed. The part of Panel

253   1 with Anode A1, A2, and A3 is labelled as Part A1, A2, and A3, respectively [see Panel 1 in

254   Figure 3(b)]. The rebars in Panel 1 were connected using three numbers of three types of

255   anodes, labeled A1, A2, and A3 (a total of 9 anodes). The anodes were tied to rebars with a

256   c/c distance of 400 mm [see Figure 3(a)]. Note that the anodes were electrically disconnected.

257   The difference between anodes A1, A2, and A3 is the surface area of the metal piece. The

258   surface area of metal pieces in A1, A2, and A3 were $\times$1, $\times$2, and $\times$4 the surface area of Anode

259   A1, respectively (see Figure 3(b)). The weight of anode metal in Anode A1, A2, and A3 were

260    $\times$1, $\times$2, and $\times$4 the weight of Anode A1, respectively. The weight (gm) to surface area of anode

261   metal (cm^2) for all anodes was 1.65. All the rebars and anodes were connected together outside

262   the panel system using electric wire and junction box, which allowed the measurement of the

263   depolarized potential of the steel 24 hours after disconnection of the anodes and the corrosion

264   rate of the steel rebars without the influence of the anodes. Panel 2 was prepared as a control

265   specimen with no anodes. Table 1 shows the mix proportions of concrete used to cast both

266   slabs. After casting, both the panels were cured with wet sack for 7 days and were exposed to

267   a natural environment within 2 km from the seashore of a coastal city in western India for 12

268   years. The panels experienced an average of 4 months per year of heavy rain and an

269   environment with relative humidity ranging from 55 to 80% for the remaining of each year and

270   temperature ranging from ≈ 15 to ≈ 35 ℃ throughout the year [40]. This created a highly

271   corrosive environment for the RC panels.

272   **Table 1 Mix proportion of concrete used to cast slabs**

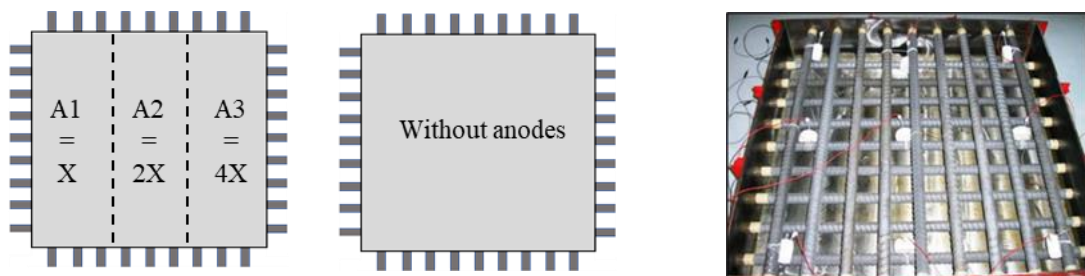| Material	Quantity (kg/m^3)
Ordinary Portland Cement	360
20 mm aggregate	683
10 mm aggregate	455
Fine aggregate	612
Water	198
NaCl	11.9

273
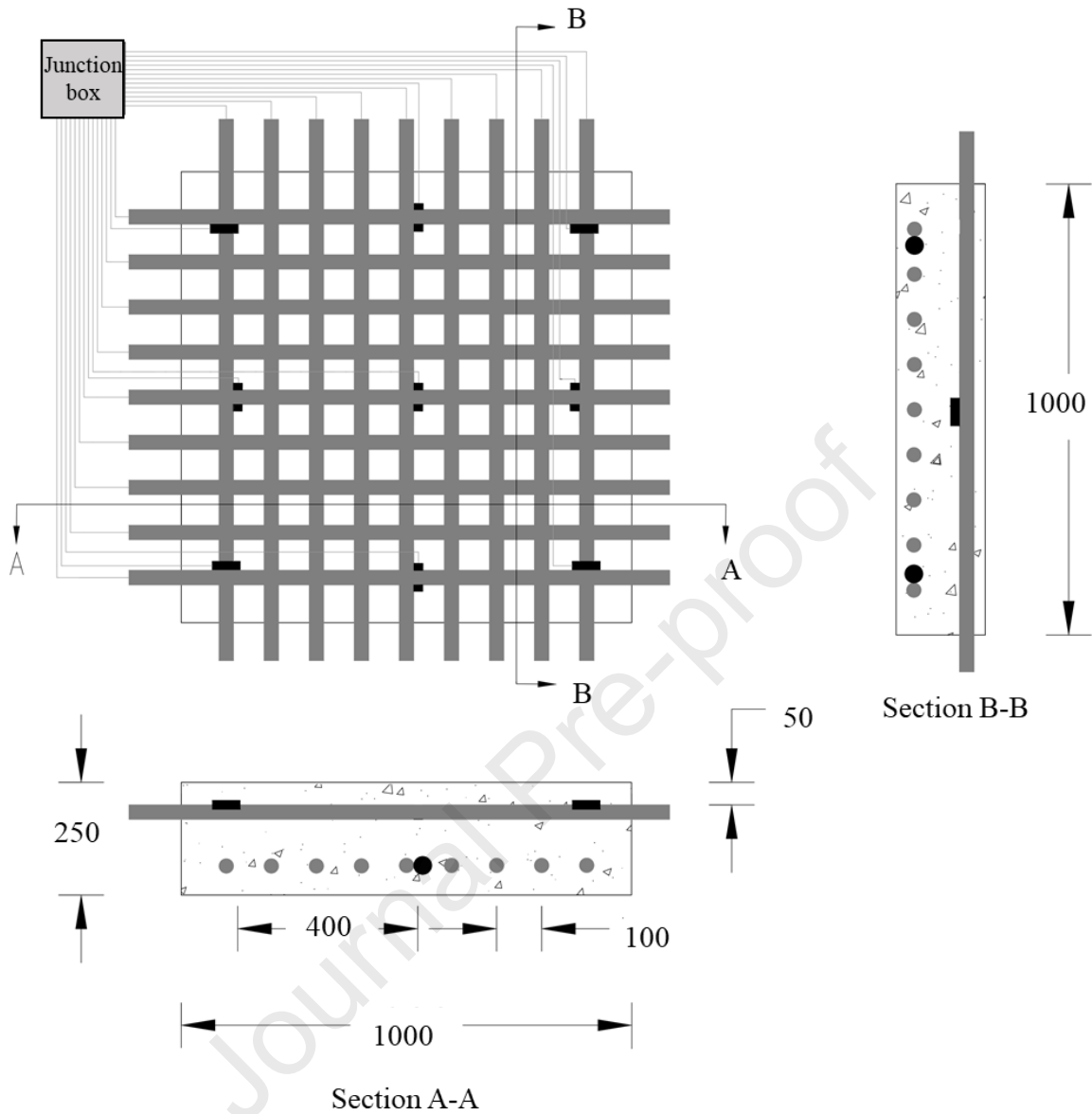
All dimensions are in mm

(a) Layout of the panel showing the position of rebars and galvanic anodes

(b) Schematic of panels with and without anodes

(c) Reinforcement cage with anodes and connecting wires before casting

274 **Figure 3: Panels schematic and photograph for assessing long-term performance of**
275 **galvanic anodes (X is the surface area of metal in Anode A1)**

276

277 ### *3.1.2 Electrochemical measurements*

278 The output protection currents from anodes were measured every month for the first

279 seven months of exposure after casting. Then, the panels were left to natural exposure for

280 about eight years. During this time, the measurements were not recorded. Then, output

281 protection current from the anodes and 24-hour depolarized potentials ($E_{24\text{-}h}$) of steel rebars

282 were measured every six months for about four years. Figure 4 shows the schematic

283 demonstrating the procedure to measure the output current from each type of anode. For this,

284 1 Ω resistor was connected in series between the anodes of each type and all the rebars. A

285 5.5 digit multimeter was used to measure the potential difference across the 1 Ω resistor.

286 Measured potential difference across the resistor was used to calculate the current using Ohm's

287 law. To measure the depolarized potential, the anodes were disconnected from the rebars for

288 24 hours. Then, the potential of each rebar was measured using a saturated calomel reference

289 electrode (SCE) positioned on the surface of the concrete directly above the measured steel

290 rebar.

291 In addition, corrosion rates of depolarized steels were measured at the end of 12 years

292 of exposure using a corrosion rate meter (see Figure 4(b)). For this, a commercially available

293 corrosion rate meter was used. The working principle of the corrosion rate meter is

294 scientifically validated and presented by Andrade and others in [41–43]. In the sensor of the

295 corrosion rate meter, the following electrodes were present: reference electrode (RE) 1, counter

296 electrode, RE 2, RE 3, and guard ring electrode. During measurements, the sensor was placed

297 on the saturated concrete surface such that RE 1, 2, and 3 were aligned in the direction of the

298 steel rebar. Each steel rebar was isolated from other steel rebars and externally connected to

299 the sensor while corrosion current density was measured. For adequate ionic conductivity, a

300 wet sponge was placed in between the sensor and the concrete surface. The potential difference

301 between the RE 2 and 3 were measured. The small potential shift (DE) is applied between steel

302   rebar and counter-electrode, which alters the potential difference between two electrodes.

303   Then, a current (I_{CE}) is applied from the guard ring until the potential between two electrode

304   returns to the original value. The current is flowing between the counter electrode and working

305   electrode in the concentrated region (i.e., confined steel surface area). Using the applied

306   potential, measured current, and Equation 1, resistance to polarization (Rp) is determined by

307   subtracting the ohmic drop across concrete (R_Ω) [44].

308    $$Rp = \left(\left(\frac{\Delta E}{I_{CE}} \right) - R_\Omega \right) \times Confined\ steel\ surface\ area \qquad (1)$$

309   *It was reported that the measured rate of corrosion in this way is only correct over a range of*

310   *half to double the recorded level* [41–43]. On the other hand, a few authors reported that the

311   calculation of corrosion rate from the corrosion rate meter is not accurate because the Stern-

312   Geary equation is not applicable for the localized corrosion, which normally occurs in RC

313   systems [45]. Therefore, it may not allow an accurate calculation of the rate of corrosion

314   [46,47]. However, *he*re, as the geometry of the slab samples is uniform. Therefore, corrosion

315   rate measurements on individual rebars can be compared.

316

| (a) output current | (b) Corrosion current density measurement using corrosion rate meter |
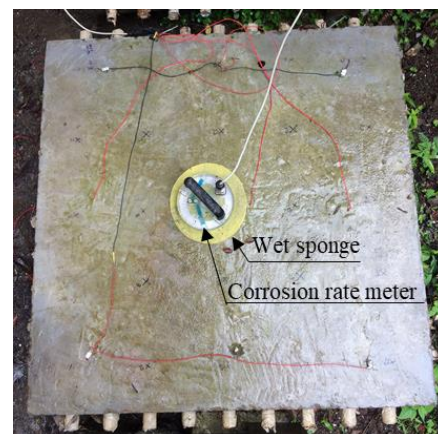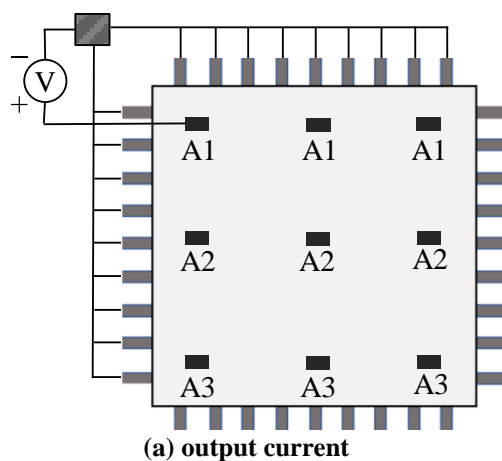
317   **Figure 4 Measurement of output current and corrosion current density**

318 **3.2   Phase II: Physico-chemical characterization of a 12-year-old galvanic anode**

319 A cylindrical concrete core containing one of the embedded anodes of Type A1 was extracted

320 from Panel 1 [see Figure 5(a)]. To understand the mechanism of activation, the anode was

321 autopsied to quantify the physico-chemical characteristics of the encapsulating mortar.

322 Samples of the encapsulating mortar were collected from three Reference Regions (RR) 1, 2,

323 and 3 [see Figure 5(b)]. Microanalytical tests were conducted to evaluate the characteristics of

324 the encapsulating mortar, which are presented next.

Note: Concrete is not shown for clarity.
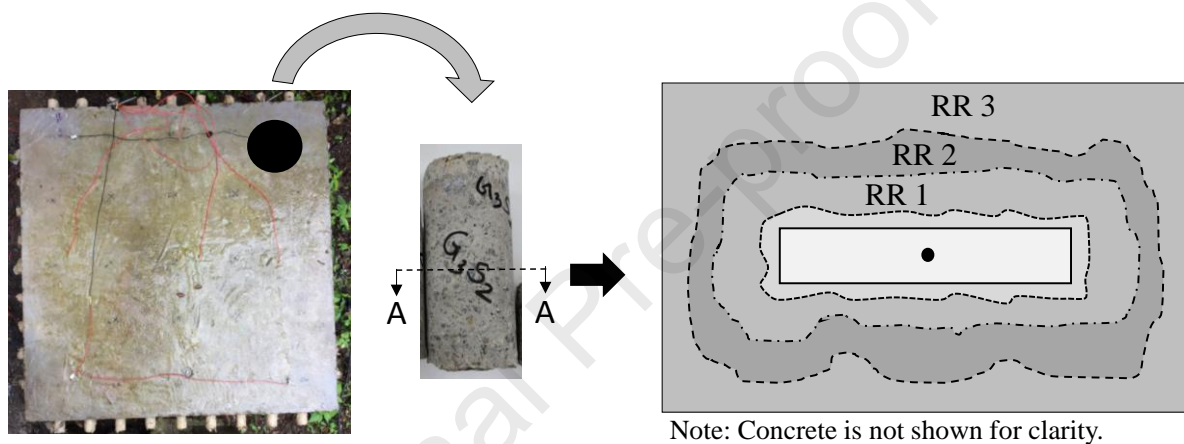
**(a) Panel 1 after extracting the cylindrical core   (b) Schematic showing feactures of galvanic anode
and extracted core with galvanic anode   after 12 years of service and reference locations**

325 **Figure 5: Procedure followed to extract the anode from Part A1 of Panel 1**

326 *3.2.1   Pore structure of encapsulating mortar*

327 The porosity and critical pore sizes of the encapsulating mortar from RR1 and RR3 were

328 determined using Mercury Intrusion Porosimetry (MIP) technique. The pore structure of

329 mortar from RR2 was not analyzed due to insufficient sample size, which was used for

330 determining the chemical composition. In this experimental program, Pascal 140–440$^{®}$ MIP

331 instrument was used to measure the pore size in the range of 100 μm to 3 nm. Three fragments

332 from the encapsulating mortar were collected from RR 1 and RR 3 with a total weight of about

333 0.3 g and thickness of each chunk ≈ 5 mm. These were used for the tests. Mercury was intruded

334 inside the pores of the chunk and the total volume of mercury intruded was used to estimate

335   the total porosity of the mortar samples. The critical pore entry diameter was the peak of the

336   differential curve of the total volume of mercury intruded.

3.2.2   Chemical composition and pH of encapsulating mortar

338   The chemical composition of the encapsulating mortar from a virgin anode and an anode after

339   12 years of service from location RR 2 were evaluated using Energy Dispersive X-ray (EDX)

340   Analysis. EDX analysis was selected because of the limitation of encapsulating mortar samples

341   obtained from the anode. In addition, acid-base titrations were performed on the samples to

342   calculate the residual lithium content and the approximate pH of encapsulating mortar in RR 1

343   and RR 3. For this, encapsulating mortar from the respective regions were ground to particle

344   size less than 100 µm. Then, approximately 2 g of ground encapsulating mortar was mixed

345   with 10 ml of de-ionized water and titrated against 1 mol/L Hydrochloric acid. The nominal

346   pH of the solution was measured using a pH electrode. A titration curve between the amount

347   of acid added and the nominal pH of solution was generated as per [19]. The amount of acid

348   required to neutralize the hydroxyl buffer in the encapsulating mortar was calculated from the

349   inflection point of the acid-base titration curves. This value was used to calculate the

350   approximate amount of lithium hydroxide monohydrate ($LiOH.H_2O$.) in the mortar sample

351   (termed as M1) as shown in Equation 4.

352    $$M1 = \frac{Volume\ of\ acid\ added \times Molecular\ weight\ of\ LiOH.H_2O}{1000} \qquad (4)$$

353   Then, the mass of lithium hydroxide as a percentage of the dried sample mass (termed as M2)

354   was calculated using Equation 5

355    $$M2 = \frac{M1}{Dry\ weight\ of\ the\ sample} \times 100 \qquad (5)$$

356   The mass of $LiOH.H_2O$ in the sample per 1000 ml of water (termed as M3) was calculated

357   using Equation 6

358    $$M3 = \frac{M2}{Evaporable\ water\ content\ of\ the\ sample} \times 100 \qquad (6)$$

359   To determine the evaporable water content, the encapsulating mortar from location of interest

360   was grounded and weighed (w1). Then, this sample was placed in the oven at a temperature

361   of 105-110ºC for 24 hours. Then, it was placed in deciccator until it cools, then weighed again

362   (w2). The difference in weight (w1-w2) is the evaporable water content of the sample. The

363   mass of one mole of $LiOH.H_2O$ is 42. The approximate pH of the mortar samples was

364   determined using Equation 7

365     $$Approximate\ pH = log\left(\frac{M3}{42}\right) + 14 \qquad\qquad (7)$$

366   After that, the encapsulating mortar was scrapped off from anode metal and the remaining piece

367   was dissected into four quadrants to assess the condition of the zinc and the tie-wires.

368   **4   RESULTS AND DISCUSSIONS**

369   **4.1   Phase I: Long-term exposure and electrochemical measurements of panel**
370   **specimens**

371   *4.1.1   Depolarized corrosion potentials*

372   Figure 6 shows the 24-hour depolarized corrosion potentials (E_{24-h}) of rebars in Panel 1 and the

373   free corrosion potential of rebars in Panel 2 with reference to saturated calomel electrode

374   (SCE). Note that all the rebars are interconnected when E_{24-h} or free corrosion potentials are

375   measured. The depolarized corrosion potentials were measured from 9 years after installation

376   of anodes until 12 years, a period that consisted of severe environmental conditions. During

377   this time, the average E_{24-h} of the rebars in Panel 1 were found to be more positive than –270

378   mV_{SCE}. This indicates that the galvanic anodes have essentially protected the rebars from the

379   admixed chlorides throughout the exposure period of 12 years. In additon, 48-hour depolarised

380   potentials were also measured. However, the depolarised potentials were within the range of

381   typical scatter of half-cell potential measurements. Therefore, further depolarised potentials

382   were not measured and anodes were connected again to the rebars. The depolarised potentials

383   more positive than −270 mV$_{SCE}$ is also justified by the output protection current, which is

384   presented later in this paper.
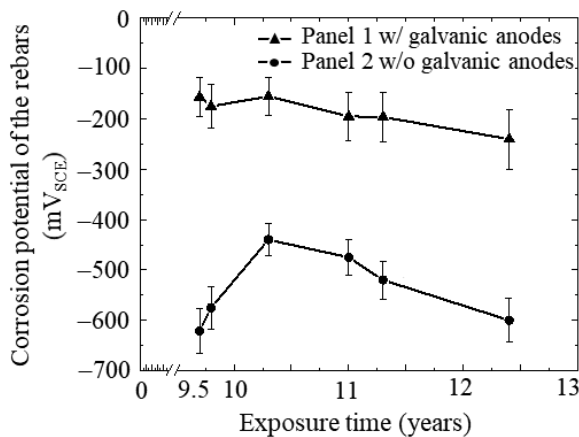
385
386   **Figure 6: Depolarized potential of rebars embedded in concrete panels**

387   On the other hand, at the end of 8 years, the free corrosion potentials of the rebars in

388   Panel 2 were found to be more negative than −600 mV$_{SCE}$. Also, Panel 2 suffered from hairline

389   cracks parallel to the rebars. This indicates that the rebars were corroding. Later, the crack

390   width kept increasing due to radial pressure exerted by more corrosion products filling in the

391   steel-concrete interface. At the end of 10 years, the crack width on the concrete surface was

392   measured to be about 2 mm, which is significantly high. Also, measured corrosion potentials

393   were more negative than −500 mV$_{SCE}$ — indicating active corrosion.

394   *4.1.2   Corrosion current density of steel rebar with and without galvanic anodes*

395   Figure 7 shows the average corrosion current density at the end of 10 years, which indicates

396   the rate of corrosion. For the top rebars in depolarized conditions of Panel 1 the corrosion

397   current density was found to be relatively insignificant ($\approx$ 0.25 μA/cm^2) and for the free

398   corroding conditions of Panel 2 the corrosion current density was on average around

399   80 μA/cm^2. The insignificant corrosion rate of the rebars of Panel 1 clearly show that they

400   were protected by the galvanic anodes. To the contrary, the rate of corrosion of the rebars of

401   Panel 2 indicates that the rebars were experiencing severe corrosion in the same exposure

402   environment as Panel 1. Therefore, the results on the rate of corrosion indicate that if the

403   number and location of anodes are adequately designed, the rebars can be protected for the

404   long term (say, more than 10 years). Number and location of anodes are designed based on the

405   corrosion conditions of individual locations considering the rate of corrosion of rebars, chloride

406   concentration in the concrete, electrical resistivity of the concrete in the location of interest,

407   steel density, etc. Note that the rate of corrosion of the bottom rebars could not be measured

408   due to the inaccessibility of the rebars.
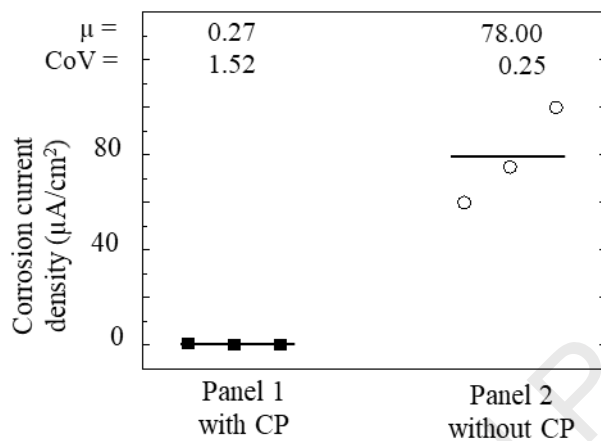
409
410   **Figure 7 Corrosion current density of the rebars at the end of 10 years after installation**
411   **of anodes**

412   The average corrosion current density of the rebars in Part A1, A2, and A3 of Panel 1

413   were found to be 0.75, 0.05, and 0.015 $\mu A/cm^2$. This indicates that the level of passivation of

414   rebars were proportional to the surface area of the anode metal pieces i.e., A3 > A2 > A1. The

415   influenced region of the panel from each anode was not estimated as it is out of the scope of

416   this paper but a spacing of 400 mm was seen to have allowed adequate protection of all the

417   steels. The corrosion current density of rebars in parts with A2 and A3 anodes were found to

418   be less than 0.1 $\mu A/cm^2$, which shows that the rebars in parts with A2 and A3 were passivated

419   as per NACE SP0290. However, the corrosion current density of one of the rebars in Part A1

420   was > 0.1 $\mu A/cm^2$, which indicates that the anode connected in Part A1 to the rebar may not

421   have sufficient surface area to supply the required protection current to passivate the whole

422   length of the steel rebars. Therefore, the efficiency of anodes was evaluated by measuring the

423   output current from anodes, which is discussed next.

424   ### *4.1.3   Effect of surface area of anode metal on performance of galvanic anode*

425   The rectangular, circular, and triangular markers in Figure 8 show the average output current

426   obtained from Anode sets A1, A2, and A3, respectively. The initial average output current

427   from anodes of Type A1, A2, and A3 was about 900, 2,000, and 3,700 µA, respectively. As

428   expected, the output current density from the anodes was proportionally higher as the surface

429   area increased. Note that the output currents were in the same ratio as the surface area of metal

430   in the galvanic anodes (A1:A2:A3 = 1:2:4). As a consequence, anodes with the higher surface

431   area were able to supply a higher current to the steel rebars. Therefore, the higher current

432   output anodes will be expected to control the rate of corrosion of the steel sooner and easier

433   than the anodes with the lower surface area. During initial exposure period (between 0 to 3

434   months), the output currents were found to be significantly decreasing. This can be attributed

435   to following two factors: (i) the hydration of concrete – leading to maturity of concrete and

436   increase in the resistivity of concrete and (ii) the surface of steel would have been active.

437   Therefore, due to high demand and low electrolyte resistance the output currents were high. In

438   about 2 to 3 months, the output current decreases exponentially for these types of anodes, then

439   stabilised [23]. The significant decrease and stabilization of output current may also have been

440   due to the build-up of the passivating oxide film on the surface of the steel rebars during their

441   early protection and from the continued hydration of the concrete, which would have resulted

442   in higher resistivity. The rate of decrease of output current was gradual from Year 1 to Year

443   12 (from about 200 days to 3700 days) after the installation of the anodes. Beyond the early

444   rapid reduction, the current density is expected to be halved over constant time periods, which,

445   for Anode A1, the aging factor (or half-life) appears to be 8.5 years. For Anodes A2 and A3,

446   the aging factor appears to at least 13 years.The average surface electrical resistivity of concrete

447   at 10- and 12-year age was found to be ≈17 kΩ·cm with coefficient of variation of 0.21. This

448   timescale of halving of the current output was termed the 'Aging Factor' elsewhere [19,48].

449   Note that the duration during early rapid reduction of output current should be eliminated for

450   calculation of Aging factor.

451
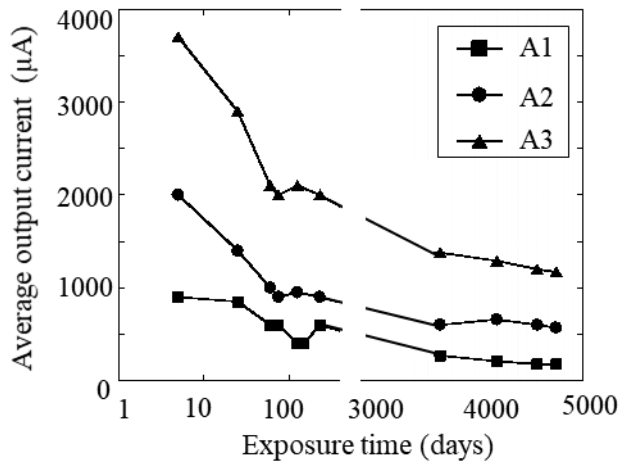
452
453   **Figure 8: Output current density from anodes showing that the anodes are in working**
454   **condition even after 12 years or more**

455   *4.1.4   Visual inspection of panels after 12 years of natural exposure*

456   Visual inspection, depicted in Figure 9(a) shows that Panel 1 did not crack after 12 years of

457   exposure to warm and humid environment even though it contained high chloride levels. The

458   black lines in the photograph of Panel 1 are the wires used for electrical connection between

459   the various anode and the rebars.   The absence of cracks indicates that the anodes had

460   successfully protected the steel from rebar corrosion even though the current density decreased

461   with time.   To identify why the current output had reduced with time, some microanalytical

462   studies were conducted, which are discussed later. As shown in Figure 9(b), Panel 2 suffered

463   from significant cracking (see black lines drawn parallel to the crack on concrete). Figure 9(b)

464   shows the closeup of the top view of the crack on Panel 2 of the concrete surface – indicating

465   that unprotected reinforced concrete structures with chloride contamination can undergo

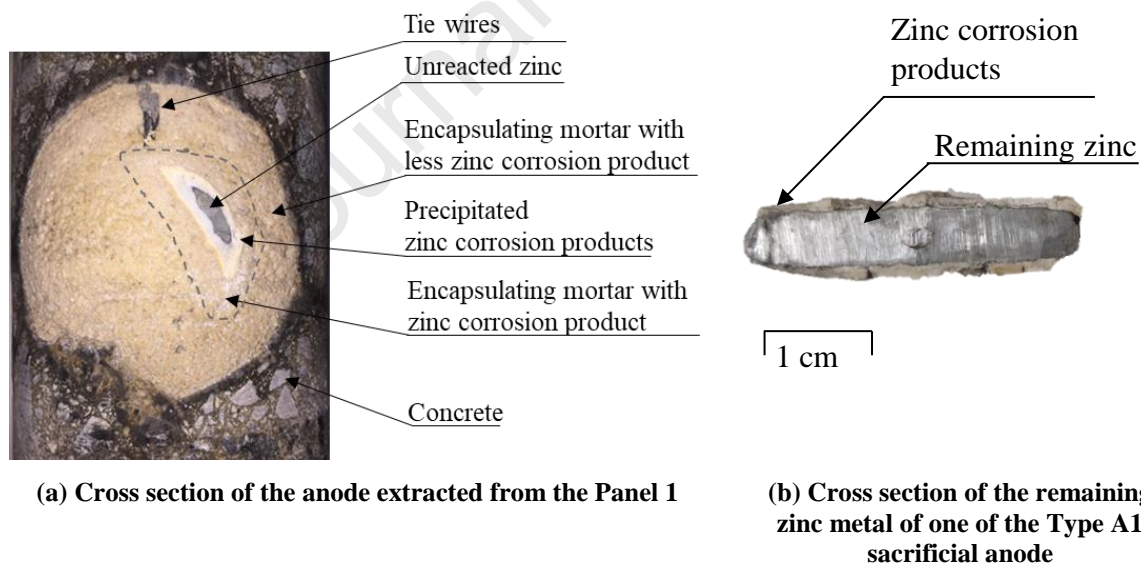466   significant corrosion, cracking, spalling, and damage.

(a) Panel 1 (with CP system)   **(b) Panel 2 (without CP system) and closeup of crack in Panel 2**
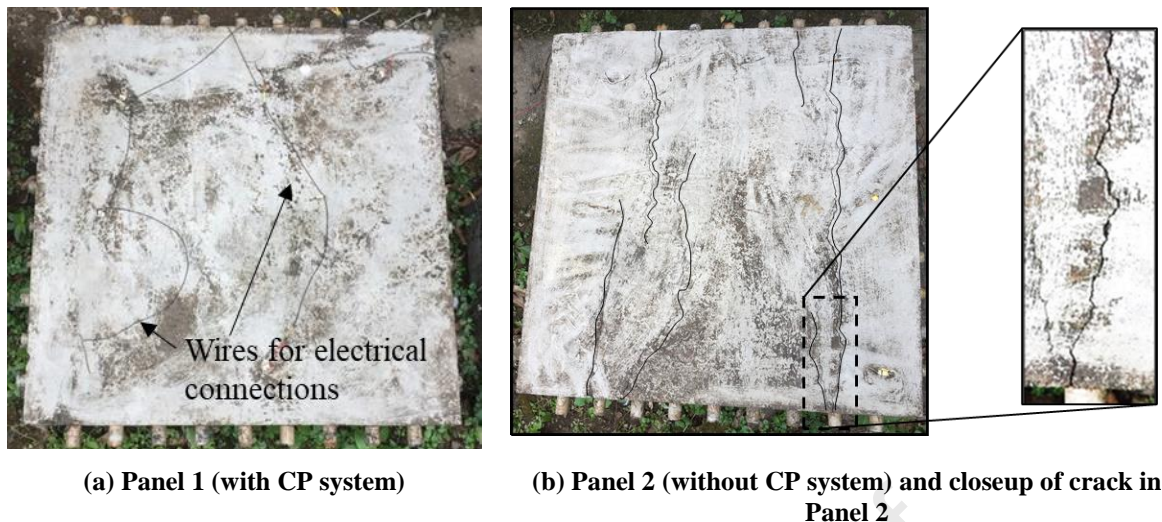
467 **Figure 9: Photograph showing the condition of the panels after 12 years of exposure.**
468 **Panel 2 shows severe corrosion**

469 **4.2**   **Phase II: Physico-chemical characteristics**

470 *4.2.1*   *Visual observation of the autopsied galvanic anode*

471 Figure 10(a) shows the curved surface area of the cylindrical concrete core extracted from

472 Part A1 of Panel 1. A part of the anode was cut during coring as the precise location of the

473 anode was not known. As expected, the unreacted zinc metal was found to be surrounded by

474 a layer of white zinc corrosion products (zinc oxides/hydroxides). Also, it was observed that

475 the zinc corrosion products had penetrated radially outwards into the encapsulating mortar until

476 about half of the width surrounding the zinc metal piece. The porous encapsulating mortar

477 could provide a path and facilitate the movement of corrosion products away from zinc metal

478 — exposing the unreacted zinc surface and providing the contact of zinc metal to the

479 encapsulating mortar with high pH, which is discussed later. Figure 10(b) shows a cross-

480 section of the unreacted zinc metal piece surrounded with yellow, dense, insoluble zinc

481 corrosion products. In the absence of adequate moisture or relative humidity, zinc corrosion

482 products can be highly resistive and interrupt the ionic conduction, which may result in

483 premature failure of galvanic anodes. Approximately $1/4^{th}$ of the thickness of zinc metal was

484 found to be consumed in about 12 years of service – indicating that if the electrical connections

485 and corrosive environment for the galvanic anode is adequate, the anode could protect the steel

486   in Panel 1 for several more years, which will depend on the characteristics of encapsulating

487   mortar and electrical connection between tie wires & zinc metal. Similarly, Dugarte and

488   Sagüés [49] reported that the anodes stop functioning due to encapsulating mortar surrounding

489   to galvanic metals failing to provide the adequate environment for continuous corrosion after

490   about 1/4th of the galvanic metal is consumed. Note that the anode used for this investigation

491   was extracted from the corner of the specimen, where it supplied current to less surface area of

492   steel than other anodes (say, those more in the middle). Therefore, the investigated anode may

493   be less consumed than other anodes. However, the rate of corrosion of depolarised steels and

494   output current density from anodes showed that the anodes are still functioning. The

495   anticipated performance of anodes in present study is discussed later based on the

496   characteristics encapsulating mortar, tie wires, and electrical connection between tie wires and

497   zinc metal.

(a) Cross section of the anode extracted from the Panel 1   (b) Cross section of the remaining zinc metal of one of the Type A1 sacrificial anode

498 **Figure 10: Condition of the galvanic anode after 12 years (the encapsulating mortar is**
499 **scraped off exposing the bare metal)**

500 *4.2.2   Critical pore size and porosity*

501   Figure 11 shows that the $d_{critical}$ for the encapsulating mortars from RR 1 and RR 3 was found

502   to be 0.1 and 1 µm, respectively. $d_{critical}$ is the maximum pore diameter that can connect the

503   largest interconnected pores. It was found that $d_{critical}$ at RR 1 was about 10 times less than

504   $d_{critical}$ of the mortar from RR 3 – indicating that a large volume of pores in RR 1 may have

505   been filled with in-soluble zinc corrosion products. Porosity is defined as the ratio of the

506   volume of pores in the encapsulating mortar sample to the total volume of the sample. The

507   design porosity of the encapsulating mortar is ≈ 20 %. The remaining porosity in RR1 and

508   RR3 were ≈2% and 8%, which is ≈90% and 60% less than the designed porosity. The porosity

509   of RR1 was ≈4 times lesser than the porosity of the encapsulating mortar in RR 3. The

510   difference in the reduction of porosity can be due to the accumulation of the insoluble zinc

511   corrosion products precipitating in the pore spaces. The zinc corrosion products get

512   precipitated hence they build up more strongly close to the zinc metal. Therefore, if an

513   adequate porosity is not provided in the encapsulating mortars, it can lead to clogging of the

514   pore and can result in the deactivation of zinc metals due to reduced alkalinity in the vicinity

515   of the zinc metal. In alkali activated galvanic anodes such as these ones, soluble zincate

516   corrosion products are produced according to Equations 8 and 9. Their solubility allows them

517   to move into the pores of the encapsulating mortar where they precipitate out as zinc oxide

518   once supersaturation occurs. It is important, therefore, that enough porosity is present in the

519   encapsulating mortar to allow percolation of the soluble corrosion products and avoid excessive

520   blockage just at the zinc/mortar interface.

521   $Zn + 2OH^- \rightarrow Zn(OH)_2 + 2e^-$ (8)

522   $Zn(OH)_2 + 2OH^- \rightarrow Zn(OH)_4^{2-}$ (9)

523
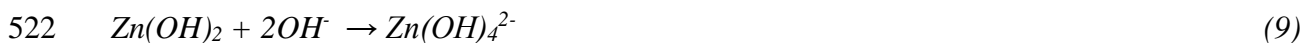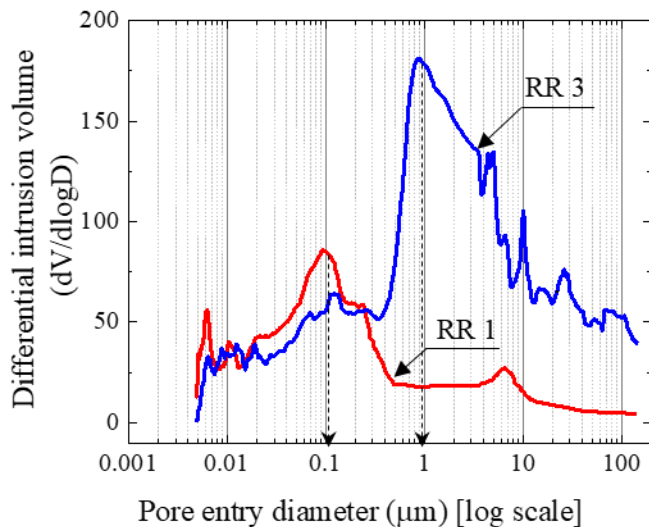
Figure 11: Pore structure of the activating mortar at RR 1 and 3 determined using Mercury Intrusion Porosimetry (each curve is the average of three samples)

4.2.3   Chemical composition of the activating mortar and residual pH

Table 2 shows the chemical composition of the encapsulating mortar collected from the virgin anode and from RR 2 of the anode extracted from the Panel after 12 years of service. Elements like Mg, Al, Si, and Ca were found during the investigation. – Compounds of these elements might have been added to facilitate the encapsulating mortar with following (i) high ion exchange and (ii) long-term corrosive environment to prevent the passivation of the zinc. For example, calcium chloride, potassium acetate, potassium hydroxide, bentonite, and gypsum are used as humectants to maintain the humidity level in the galvanic anode [30,50,51]. Lithium hydroxide was used as activator [52]. Here, the total concentration of elements (Mg, Al, Si, Ca, Zn, O, K, and Fe) in encapsulating mortar from virgin anode was found to be about 75%. The remaining would have been Li concentration, which could not be detected because the atomic weight of Li is 6.9 g/mol, which is less than C (12.0 g/mol), which is the lightest element that can be determined by the instrument. On the other hand, the concentration of these elements in encapsulating mortar from anode after 12 years of service was found to be 100% - indicating that Lithium hydroxide get consumed and lithium migrates out of encapsulating mortar during the process to provide alkaline environment to the zinc metal.

542   Simultaneously, the concentration of chlorides was found to increase from 0 to 3.78% due to

543   migration from concrete to encapsulating mortar. The concentration of a few of the elements

544   such as Mg, Al, and Si were found to be increasing (from-to) 0.26-4.52, 6.31-16.33, and 2.37-

545   18.86, respectively. The concentration seemed to increase, which is misleading as the lithium

546   has migrated out and the powder used does not contain Li. The concentration of LiOH was

547   determined using the titration method, which is presented later.

548   **Table 2: Chemical composition of encapsulating mortar at RR 2**

| Element	Weight (%)	
	Virgin galvanic anode	**Galvanic anode post 12 year of service**
Mg	0.26	4.52
Al	6.31	16.33
Si	2.37	18.86
Cl	0.0	3.78
Ca	12.59	11.91
Zn	1.75	0.69
O	50.69	43.91
K	0.34	0
Fe	0.3	0
Li	Could not be detected using EDX.	

549

550   After 12 years of service, traces of chlorides were found in the encapsulating mortar.

551   The presence of chlorides might be due to the diffusion or electromigration of the chloride ions

552   from the contaminated concrete through the encapsulating mortar towards the

553   electrochemically positive anode metal. The concentration of zinc was also found less than

554   that of the virgin anodes. This can be attributed to dissolution of zinc corrosion products and

555   their migration away from the zinc metal in the encapsulating mortar. In other words,

556   availability of zinc in virgin encapsulating mortar was present in the encapsulating mortar (in

557   region RR2) due to contamination during the manufacturing process. During the cathodic

558   protection process, the anions produced at the cathodic sites (say, OH^-) may migrate towards

559   the zinc metal. During this migration, they might react with the zinc to from soluble zincate.

560   Then, these zincate ions may have got diffused outwards away from RR2. This process

561 continues till the supersaturation state is achieved. This exchange of ions can alter the

562 functionality of galvanic anodes. For example, if zinc corrosion products get filled in the pores

563 of the encapsulating mortar at the zinc-encapsulating mortar interface, then the fresh zinc metal

564 will not be adequately exposed to the activating materials in the encapsulating mortar. Also,

565 due to filling of pores, the availability of humectants at the zinc metal surface can get reduced

566 – leading to difficulty in maintaining a high humid micro-climate at zinc-encapsulating mortar

567 interface, which can reduce the rate of corrosion of zinc. Also, the concentration of lithium

568 was found to be decreasing from the location close of anode metal, which is presented next.

569 Such alteration in characteristics of the anode can reduce the efficiency of galvanic anodes.

570 The acid-base titration curve was used to determine the approximate pH buffer of the

571 encapsulating mortar in one of the samples. The approximate amount of LiOH and the pH

572 buffer was calculated by using Equations 2 to 5. The solubility of $LiOH.H_2O$ in water at 20º

573 C is approximately 22.0 g/100 cc of water [53]. The value of $LiOH.H_2O$ determined at the

574 RR 2 and RR 3 was found to be 17 and 22 g per 100 ml of water, which is more than the

575 solubility of $LiOH.H_2O$ (220 g/l of water). This indicates that there is an excess LiOH in the

576 samples, which will buffer the solution at a calculated pH of about 14.4. The value of

577 $LiOH.H_2O$ determined at the RR 1 was found to be ≈ 1 g per 100 ml of water – indicating the

578 reduction in the concentration of LiOH due to the reduced alkalinity of the mortar around the

579 anode metal. The approximately calculated pH at this region was determined using Equation

580 5.

581 Figure 12 shows that the calculated pH of encapsulating mortar in RR 1, 2, and 3 were

582 found to be 14.1, 14.4, and 14.4, respectively. At Region 2 and 3, the concentration of LiOH

583 was found to be greater than 220 g/l of water, indicating that there is excess LiOH in the sample

584 which will buffer the solution at around pH 14.4. Therefore, the decrease in the pH buffer at

585 RR1 can be due to the consumption of OH^- locally and electromigration of Li^+ away from the

586 zinc, eventually reducing the level of LiOH to below saturation. However, the decrease in pH

587   from 14.4 to 14 after 12 years of service may not be large enough to significantly alter the

588   functionality of the galvanic anode. This continued good performance of the anodes can be

589   attributed to the high pH and adequate porosity of the encapsulating mortar, which can maintain

590   activity of the zinc metal and provide the path for the diffusion of soluble corrosion products
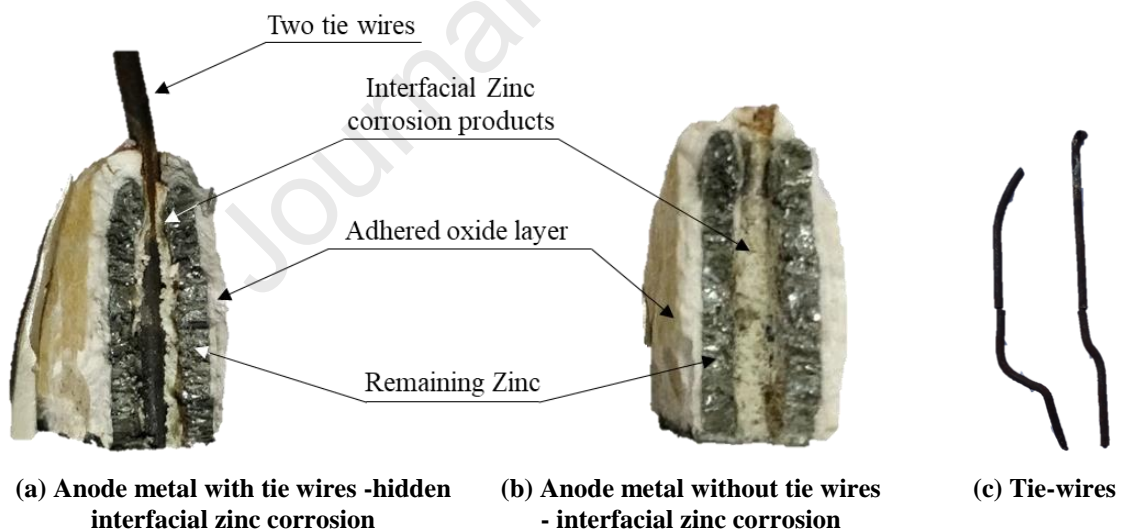
591   away from the interface.
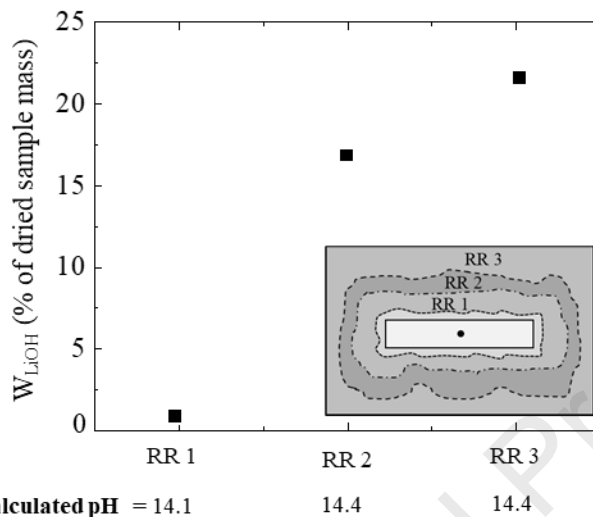
592
593   **Figure 12: Residual pH and lithium hydroxide content of the encapsulating mortar in**
594   **Reference Regions 1, 2, and 3**

595   *4.2.4   Electrical connection between zinc metal, tie wire, and rebars*

596   Figure 13 shows the photograph of the interface of the autopsied galvanic anode and tie wires.

597   Figure 13(a) shows that a layer of adherent insoluble zinc corrosion product was formed

598   surrounding to the zinc metal surface. The corrosion products of zinc occupy the space vacated

599   by the zinc metal and a part of it diffuses or migrates into the encapsulating mortar. In absence

600   of moisture, the adherent semi-conductive zinc oxide layer can act as an increased barrier to

601   the ionic conduction process [27,54], thereby decreasing the efficiency of the galvanic anodes

602   in supplying electrons. Also, Figure 13(a) shows the fractured surface of the anode metal piece.

603   The tie wires had zinc corrosion products surrounding them, with a very small region left with

604   an electrical connection to the zinc metal. Figure 13(b) shows the fractured cross-section of

605   zinc metal without the tie wires, where zinc corrosion product (white in color) are visible.

606   Figure 13(c) shows that the two tie wires were die cast at the time of manufacturing. The use

607   of two tie wires close together may allow a space between them where molten zinc cannot

608   penetrate. During the service life of anodes, moisture may enter into this space. Therefore, a

609   galvanic cell can form between the zinc and tie wires. In this case and generally, tie wires are

610   made of more electropositive metal than galvanic metal. Therefore, the zinc can corrode and

611   form a layer of corrosion product surrounding the tie wire. In the rare event, this zinc oxide

612   layer can completely cover the tie wires embedded in anode metal (zinc). Then, electric

613   connection between the zinc core and the tie wires may be lost. Zinc oxide, being a semi-

614   conductor, will become more conductive in the presence of moisture and allow the flow of

615   current [54,55]. Therefore, without moisture at the interface, the galvanic anode may not

616   adequately protect the structure if the electrical connection between the zinc metal and tie wires

617   is lost. With this learning, diecasting the zinc metal or zinc alloy on a single tie wire or well

618   separated tie wires are recommended.

(a) Anode metal with tie wires -hidden interfacial zinc corrosion   **(b) Anode metal without tie wires - interfacial zinc corrosion**   **(c) Tie-wires**

619   **Figure 13 Condition of anode metal (zinc) at the end of 12 years**

620   In addition, the material of tie wire can also affect the long-term performance of

621   galvanic anodes. For example, mild steel tie wires can undergo surface corrosion during

622   transportation and storage of galvanic anodes. Also, at repair sites, mild steel tie wires are tied

623   to the steel rebars and left tied to steel rebars until the repair concrete is placed. During this

624   time, the tie wires undergo surface corrosion [56]. At the time of installation, the electrical

625   contact between the steel reinforcement and the tie wires (through the surfaces) should be

626   ensured. At the time of installation, the rust from the tie wires will get exfoliated due to the

627   abrasion, tying, and twisting processes. Therefore, it would get sufficient contact for electronic

628   conduction. After that, both tie wires and steel rebars gets cathodically protected. If galvanic

629   anodes are not installed with abrasion, tying, and twisting processes, the rust layer on tie wires

630   of the galvanic anodes may hinder the supply of electrons to the steel rebars as expected.

631   Considering this, galvanic anodes with corrosion-resistant metal tie wires (e.g., stainless steel)

632   can be a good replacement for mild steel tie wires. Towards this, either the electrical

633   connections should be checked just before placing the concrete or tie wires made of corrosion-

634   resistant materials (say, stainless steel tie wires) should be used [57]. In short, anodes with

635   corrosion-resistant, well-separated tie wires or anodes with corrosion-resistant single tie wire

636   should be selected for cathodic protection.

637   *4.2.5   Proposed mechanism of degradation of galvanic anode systems*

638   Figure 14 shows a possible degradation mechanism of galvanic anodes. Figure 14(a) shows a

639   virgin galvanic anode consisting of uncorroded zinc metal, two closely placed tie wires, and

640   encapsulating mortar with interconnected pores. After several years of service and corrosion

641   of the zinc metal, Figure 14(b) shows that some of the zinc corrosion products can diffuse or

642   migrate into the interconnected pore structure of the encapsulating mortar, and some corrosion

643   products will simply fill the space vacated by the corroding zinc metal [see the zoomed image

644   in Figure 14(b)]. The movement of the zinc corrosion product exposes the fresh zinc metal

645   surface to the high pH of encapsulating mortar – helping to ensure the continued corrosion of

646   zinc metal. If the porosity and interconnectivity of pores is not sufficient to expose the zinc

647   metal, the effectiveness of the anode may decrease due to reduced ionic conductivity between

648   zinc metal and the corroding rebars. In addition, the gap between two tie wires and between

649   tie wire and the zinc metal may allow moisture to enter and result in interfacial corrosion of

650   zinc metal [see the zoomed image in Figure 14(b)]. Once the corrosion products cover the tie

651 wires and no moisture is available to provide electrical connection between them, the galvanic

652 anode activity may decrease [54,55].

(a) Virgin galvanic anode   (b) galvanic anode after long-term service
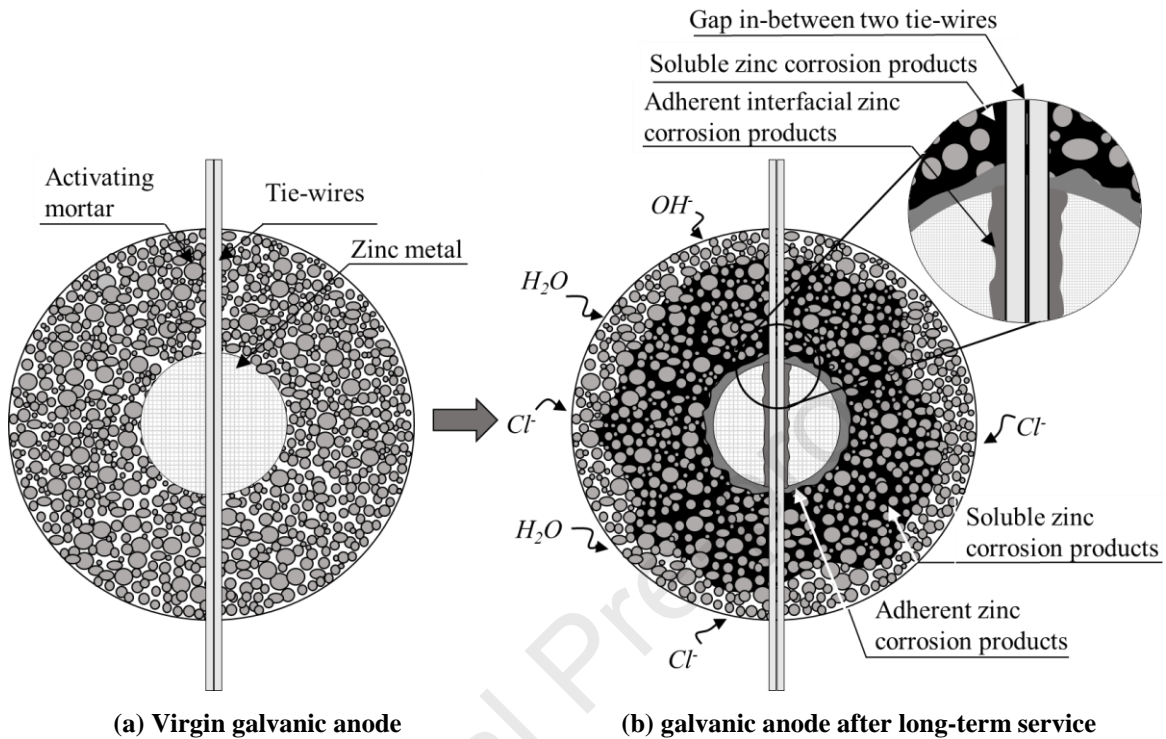
653 **Figure 14: Schematic showing the physico-chemical interactions in the encapsulating**
654 **mortar**

655 **5 RECOMMENDATIONS FOR DESIGN OF GALVANIC ANODES**

656 Based on the 12-year long performance assessment of the galvanic anodes and microanalytical

657 studies on the galvanic anode, following are the recommendations to design durable for design

658 of galvanic anodes in RC systems:

659 • Mass of the galvanic anode metals alone does not define their efficiency. The mass of

660 galvanic anode metals can define how long the galvanic anodes can deliver current to

661 the steel rebars, but the level of current will be governed by the design surface area of

662 galvanic anode metals. Therefore, specifications should include considering both

663 surface area of galvanic anode metals and the mass of the galvanic anode metals. The

664 most important consideration is that sufficient current is provided over the design

665 service life of the anode. Therefore, specifications considering the ratio of mass of

666 galvanic anode metal (g) to the surface area of galvanic anode metal (cm^2) with

667   minimum mass of anode metal can be introduced as one of the specifications. However,

668   more research is required to propose an adequate ratio of mass and surface area of

669   anode. However, the long-term level of current can be determined by knowledge of the

670   'Aging Factor' of the anode which defines the number of years required for the current

671   output of the individual anode to be halved.

672   •   An elevated pH of the encapsulating mortar keeps the galvanic metal active. In another

673   publication [19], the output current from the galvanic anode was found to reduce when

674   the pH of encapsulating mortar was less than 13.8. In this research, the pH at zinc-

675   encapsulating interface was found to be 14.1, which can still help the zinc to corrode.

676   Considering results from [19], the concentration of the activator should be chosen such

677   that the pH of encapsulating mortar is >13.8 and preferably >14 throughout the service

678   life of galvanic anode.

679   •   The pore structure in combination with the high pH environment which allows the

680   zincate corrosion products to remain soluble, helps to accommodate the corrosion

681   products of the galvanic metal. Therefore, minimum porosity of the encapsulating

682   mortar should be designed and, according to recent estimates, should be > 20% of

683   volume of encapsulating mortar (≈ 200 mm^3/g). In this research, it was found that the

684   adequate diffusion or migration of corrosion products was possible when the

685   encapsulating mortar have the critical pore size ($d_{critical}$) in the range of 5 to 15 µm. A

686   higher $d_{critical}$ may be an advantage as the current output was seen to diminish with time,

687   but more work is required to establish $d_{critical}$ and total pore volume of the encapsulating

688   mortar.

689   •   To avoid formation of a rust layer on the tie wires during transportation, storage, and

690   placement, corrosion-resistant materials such as stainless steel should be used for tie

691   wires.

692   •   To avoid corrosion at the interface of adjacent embedded lengths of the tie wires and

693   the galvanic anode metal, the anode metal should be diecast around well-separated (say,

694   at least 0.5 mm apart) corrosion-resistant tie-wires or a single tie wire. Furthermore,

695   the tie-wires should not be attached to the anode metal either by welding or other means.

696 • The resistance between tie wire and the rebar onto which the anode is attached should
697 not be more than 1 Ω. This should be established during the installation of the anode.

698 Table 3 summarizes the recommendations for the selection of galvanic anodes.

699 **Table 3 Proposed specifications of galvanic anodes**

Characteristic/parameter	Recommended specification
Maximum ratio of mass of galvanic anode metal (g) to the surface area of galvanic anode metal (cm^2)	To be decided based on aging factor, which can ensure to provide sufficient current is provided over the targeted service life of the anode.
Minimum calculated pH throughout the service life of galvanic anode	13.8
Minimum porosity of encapsulating mortar	20 % of the total volume of encapsulating mortar
Critical pore size	Minimum 5 µm. To decide the upper limit, more research is required.
Material of tie wire	Stainless steel or similarly corrosion-resistant steel
Minimum distance between tie wires (if more than 1 tie wire is used)	0.5 mm
The connection between anode metal and tie wire(s)	• Any method which can aggravate the corrosion is prohibited. For example, welding of tie wire and galvanic anode metal is not allowed • Electrical connections between the anode metal and the steel reinforcement should be ensured until the full consumption of the galvanic anode metal.

700

701 **6   SUMMARY AND CONCLUSIONS**

702 The 12 year-long performance of galvanic anodes was assessed using two reinforced concrete

703 panel specimens with and without anodes with 2% chloride ion by mass of binder added. For

704 this, electrochemical measurements, such as depolarized corrosion potential, output current,

705 and corrosion current density, were performed. The results indicate that the galvanic anodes

706 were able to passivate the steel reinforcement even in highly aggressive warm and humid

707 environments for about 12 years. With adequate design and intact electrical connections, the

708 cathodic protection approach is expected to mitigate reinforcement corrosion in similar

709 environments (concrete with chlorides) for about 10 to 15 years. This duration can be longer

710 when adequately designed durable galvanic anodes are installed to rebars without corrosion or

711 not sufficient chlorides in the vicinity of steel rebars. The output protection current has roughly

712 halved between say Month 6 and Year 12, which indicates that an 'Aging factor' may be

713 determined, which can aid in the long-term design of the required current output.

714 After 12 years of service, microanalytical studies such as pore size distribution,

715 localized pH determinations, and chemical composition analysis of the encapsulating mortar at

716 various locations were conducted to understand the degradation mechanisms of the anodes.

717 Note that the anode used in this investigation was extracted from the corner of the specimen –

718 indicating that the investigated anode may be less consumed than other anodes. The critical

719 pore size ($d_{critical}$) in encapsulating mortar near (RR1) and away (RR3) from the anode metal

720 was found to be 1 and 10 µm. Similarly, the remaining porosity in RR1 and RR3 were ≈90%

721 and 60% less than the designed porosity, respectively. The reduction in $d_{critical}$ and porosity of

722 encapsulating mortar indicate that the zinc corrosion products diffuse/migrate away from the

723 anode metal. Therefore, adequate $d_{critical}$ can facilitate the long-term performance of galvanic

724 anodes. Further research is required to understand how the reduction in pore size will affect

725 the conductivity of encapsulating mortar. In addition, the interface corrosion of tie wire and

726 zinc metal highlights the importance of diecasting with gap between tie wires and between tie

727 wire and galvanic anode filled with galvanic anode metal. Based on these, specifications are

728 proposed to design the galvanic anodes to achieve the durable service life.

8 REFERENCES

[1] L. Bertolini, E. Redaelli, Depassivation of steel reinforcement in case of pitting corrosion: detection techniques for laboratory studies, Mater. Corros. Und Korrosion. 60 (2009) 608–616. https://doi.org/10.1002/maco.200905276.

[2] R.B. Polder, G. Leegwater, D. Worm, W. Courage, Service life and life cycle cost modelling of cathodic protection systems for concrete structures, Cem. Concr. Compos. 47 (2013) 69–74. https://doi.org/10.1016/j.cemconcomp.2013.05.004.

[3] D. Kamde, R. Pillai, Effect of sunlight/ultraviolet exposure on the corrosion of fusion bonded-epoxy (FBE) coated steel rebars in concrete, CORROSION. (2020). https://doi.org/10.5006/3588.

[4] D.K. Kamde, R.G. Pillai, Effect of surface preparation on corrosion of steel rebars coated with cement-polymer-composites (CPC) and embedded in concrete, Constr. Build. Mater. 237 (2020) 1–11. https://doi.org/10.1016/j.conbuildmat.2019.117616.

[5] G. Koch, J. Varney, N. Thompson, O. Moghissi, M. Gould, J. Payer, International Measures of Prevention , Application , and Economics of Corrosion Technologies Study, 2016. http://impact.nace.org/documents/Nace-International-Report.pdf.

[6] G.P. Tilly, J. Jacob, Concrete repairs - performance in service and current practice, EN 1504 se, IHS BRE Press, Bracknell, 2007.

[7] N. Krishnan, D.K. Kamde, Z.D. Veedu, R.G. Pillai, D. Shah, V. Rajendran, Long-term performance and life-cycle-cost benefits of cathodic protection of concrete structures using galvanic anodes, J. Build. Eng. In press (2021).

[8] G. Sergi, Ten-year results of galvanic sacrificial anodes in steel reinforced concrete, Mater. Corros. 62 (2011) 98–104. https://doi.org/http://dx.10.1002/maco.201005707.

[9] C. Christodoulou, C. Goodier, S. Austin, J. Webb, G.K. Glass, Diagnosing the cause of incipient anodes in repaired reinforced concrete structures, Corros. Sci. 69 (2013) 123–129. https://doi.org/10.1016/j.corsci.2012.11.032.

[10] C. Christodoulou, C.I. Goodier, S.A. Austin, G.K. Glass, J. Webb, A new arrangement of galvanic anodes for the repair of reinforced concrete structures, Constr. Build. Mater. 50 (2014) 300–307. https://doi.org/10.1016/j.conbuildmat.2013.09.062.

[11] M.O. Kim, A. Bordelon, M.K. Lee, B.H. Oh, Cracking and failure of patch repairs in RC members subjected to bar corrosion, Constr. Build. Mater. 107 (2016) 255–263. https://doi.org/10.1016/j.conbuildmat.2016.01.017.

[12] R.B. Polder, W.H.A. Peelen, W.M.G. Courage, Non-traditional assessment and maintenance methods for aging concrete structures - Technical and non-technical issues, Mater. Corros. 63 (2012) 1147–1153. https://doi.org/10.1002/maco.201206725.

[13] K. Wilson, M. Jawed, V. Ngala, The selection and use of cathodic protection systems for the repair of reinforced concrete structures, Constr. Build. Mater. 39 (2013) 19–25. https://doi.org/10.1016/j.conbuildmat.2012.05.037.

774   [14]   F. Sandron, D.W. Whitmore, P. Eng, Galvanic Protection for Reinforced Concrete
775   Bridge Structures, (2005) 1–14.

776   [15]   L. Bertolini, M. Gastaldi, M.P. Pedeferri, E. Redaelli, Prevention of steel corrosion in
777   concrete exposed to seawater with submerged sacrificial anodes, Corros. Sci. 44 (2002)
778   1497–1513. https://doi.org/10.1016/S0010-938X(01)00168-8.

779   [16]   E. Redaelli, F. Lollini, L. Bertolini, Throwing power of localised anodes for the cathodic
780   protection of slender carbonated concrete elements in atmospheric conditions, Constr.
781   Build. Mater. 39 (2013) 95–104. https://doi.org/10.1016/j.conbuildmat.2012.05.014.

782   [17]   F.J. Presuel-Moreno, S.C. Kranc, A.A. Sagüés, Cathodic prevention distribution in
783   partially submerged reinforced concrete, Corrosion. 61 (2003) 548–558.
784   https://doi.org/10.5006/1.3278190.

785   [18]   L. Bertolini, E. Redaelli, Throwing power of cathodic prevention applied by means of
786   sacrificial anodes to partially submerged marine reinforced concrete piles: Results of
787   numerical   simulations,   Corros.   Sci.   51   (2009)   2218–2230.
788   https://doi.org/10.1016/j.corsci.2009.06.012.

789   [19]   G. Sergi, G. Seneviratne, D. Simpson, Monitoring results of galvanic anodes in steel
790   reinforced concrete over 20 years, Constr. Build. Mater. 269 (2021) 121309.
791   https://doi.org/10.1016/j.conbuildmat.2020.121309.

792   [20]   BS EN ISO 12696:2012, BSI Standards Publication Cathodic protection of steel in
793   concrete (ISO 12696 : 2012), BSI, Brussels, 2012.

794   [21]   A. Goyal, H. Sadeghi, E. Ganjian, A. Omotayo, Predicting the corrosion rate of steel in
795   cathodically protected concrete using potential shift, Constr. Build. Mater. 194 (2019)
796   344–349. https://doi.org/10.1016/j.conbuildmat.2018.10.153.

797   [22]   C. Christodoulou, G. Glass, J. Webb, V. Ngala, S. Beamish, P. Gilbert, Evaluation of
798   Galvanic Technologies Available for Bridge Structures, (2008) 10–12.

799   [23]   J.C. Ball, D.W. Whitmore, Embedded Galvanic Anodes for Targeted Protection in
800   Reinforced Concrete Structures, Cocrete Repair Bull. 22 (2009) 6–9.

801   [24]   O.T. De Rincón, A. Torres-Acosta, A. Sagüés, M. Martinez-Madrid, Galvanic anodes
802   for   reinforced   concrete   structures: A   review,   Corrosion.   74   (2018)   715–723.
803   https://doi.org/10.5006/2613.

804   [25]   D. Whitmore, M. Miltenberger, Galvanic cathodic protection of corroded reinforced
805   concrete structures, NACE - Int. Corros. Conf. Ser. 2019-March (2019).

806   [26]   R. Polder, W. Peelen, Cathodic protection of steel in concrete-experience and overview
807   of 30 years application, in: MATEC Web Conf., Int. Conf. Concr. Repair, Rehabil.
808   Retrofit., 2018: p. 6. https://doi.org/10.1051/matecconf/201819901002.

809   [27]   W. Schwarz, M. Bakalli, M. Donadio, A novel type of discrete galvanic zinc anodes for
810   the prevention of incipient anodes induced by patch repair, in: Eur. Corros. Congr.
811   EUROCORR 2016, 2016: pp. 2136–2144.

812 [28] I. Genesca, L. Betancourt, L. Jerade, C. Rodriguez, F.J. Rodriguez, Electrochemical
813   testing of galvanic anodes, Mater. Sci. Forum. 289–292 (1998) 1275–1288.
814   https://doi.org/10.4028/www.scientific.net/msf.289-292.1275.

815 [29] M.J. Dugarte, A.A. Sagüés, Sacrificial point anodes for cathodic prevention of
816   reinforcing steel in concrete repairs: Part 1-polarization behavior, Corrosion. 70 (2014)
817   303–317. https://doi.org/10.5006/1016.

818 [30] D. Whitmore, S. Abbott, Using Humectants to Enhance the Performance of Embedded
819   Galvanic Anodes, in: NACE - Int. Corros. Conf. Ser., NACE International, San Diego,
820   2003: pp. 1–9.

821 [31] N. Idusuyi, O. Oluwole, Aluminium anode activation research- a review, Int. J. Sci.
822   Technol. 2 (2012) 561–565.

823 [32] N. Khomwan, P. Mungsantisuk, Startup Thailand: A new innovative sacrificial anode
824   for reinforced concrete structures, Eng. J. 23 (2019) 235–261.
825   https://doi.org/10.4186/ej.2019.23.4.235.

826 [33] G. Sergi, G. Seneviratne, Improved design consideration for steel reinforcement
827   corrosion control with galvanic anodes following performance evaluation from analysis
828   of site data, in: Struct. Faults Repair, Edinburgh, 2021.

829 [34] J. Genescà Ferrer, J. Juárez, Development and testing of galvanic anodes for cathodic
830   protection, Contrib. to Sci. 1 (2000) 331–343.

831 [35] G. Sergi, C.L. Page, Sacrificial Anodes for Cathodic Prevention of Reinforcing Steel
832   Around Patch Repairs Applied to Chloride-Contaminated Concrete, Eurocorr 99. (1999)
833   1–9.

834 [36] W.J. Smith, F.E. Goodwin, Hot Dip Coatings, Ref. Modul. Mater. Sci. Mater. Eng.
835   (2017) 1–19. https://doi.org/10.1016/b978-0-12-803581-8.09214-6.

836 [37] G.T. Parthiban, T. Parthiban, R. Ravi, V. Saraswathy, N. Palaniswamy, V. Sivan,
837   Cathodic protection of steel in concrete using magnesium alloy anode, Corros. Sci. 50
838   (2008) 3329–3335. https://doi.org/10.1016/j.corsci.2008.08.040.

839 [38] O.T. De Rincon, A.R. de Carruyo, D. Romero, E. Cuica, Evaluation of the effect of
840   oxidation products of aluminum sacrificial anodes in reinforced concrete structures,
841   Corrosion. 48 (1992) 960–967. https://doi.org/10.5006/1.3315900.

842 [39] C. Christodoulou, C.I. Goodier, S.A. Austin, Site performance of galvanic anodes in
843   concrete repairs, Concr. Solut. - Proc. Concr. Solut. 5th Int. Conf. Concr. Repair. (2014)
844   167–172. https://doi.org/10.1201/b17394-28.

845 [40] Weather Online, (2020) 1. https://www.weatheronline.in/weather/maps/city (accessed
846   December 21, 2020).

847 [41] J.A. Gonzalez, M. Benito, S. Feliu, P. Rodriguez, C. Andrade, Suitability of assessment
848   methods for identifying active and passive zones in reinforced concrete, Corrosion. 51
849   (1995) 145–152. https://doi.org/10.5006/1.3293586.

850 [42] P.C. Andrade, C. Alonso, R. Polder, R. Cigna, O. Vennesland, M. Salta, A. Raharinaivo,
851 B. Elsener, RILEM TC 154-EMC : ' Electrochemical Techniques for Measuring
852 Metallic Corrosion ' Test methods for on-site corrosion rate measurement of steel
853 reinforcement in concrete by means of the polarization resistance method, Mater. Struct.
854 37 (2004) 623–643.

855 [43] S. Feliu, J.A. González, C. Andrade, Multiple-electrode method for estimating the
856 polarization resistance in large structures, J. Appl. Electrochem. 26 (1996) 305–309.
857 https://doi.org/10.1007/BF00242100.

858 [44] H. Wojtas, Determination of corrosion rate of reinforcement with a modulated guard
859 ring electrode; analysis of errors due to lateral current distribution, Corros. Sci. 46
860 (2004) 1621–1632. https://doi.org/10.1016/j.corsci.2003.10.007.

861 [45] S. Laurens, P. Hénocq, N. Rouleau, F. Deby, E. Samson, J. Marchand, B. Bissonnette,
862 Steady-state polarization response of chloride-induced macrocell corrosion systems in
863 steel reinforced concrete - Numerical and experimental investigations, Cem. Concr. Res.
864 79 (2016) 272–290. https://doi.org/10.1016/j.cemconres.2015.09.021.

865 [46] U. Angst, M. Büchler, On the applicability of the Stern-Geary relationship to determine
866 instantaneous corrosion rates in macro-cell corrosion, Mater. Corros. 66 (2015) 1017–
867 1028. https://doi.org/10.1002/maco.201407997.

868 [47] U. Angst, M. Büchler, A new perspective on measuring the corrosion rate of localized
869 corrosion, Mater. Corros. 71 (2020) 808–823. https://doi.org/10.1002/maco.201911467.

870 [48] D. Whitmore, G. Sergi, Long-term Monitoring Provides Data Required to Predict
871 Performance and Perform Intelligent Design of Galvanic Corrosion Control Systems for
872 Reinforced Concrete Structures, in: NACE Corros. Conf. Expo, 2021.

873 [49] M.J. Dugarte, A.A. Sagüés, Galvanic point anodes for extending the service life of
874 patch areas upon reinforced concrete bridge, 2009.

875 [50] G.R. Holcomb, B.S. Covino, J.H. Russell, S.J. Bullard, S.D. Cramer, W.K. Collins, J.E.
876 Bennett, H.M. Laylor, Corrosion 2000, (2000).

877 [51] J.E. Bennett, Activating matrix for cathodic protection, US 2009/0183998 A1, 2009.
878 http://dx.doi.org/10.1016/j.ijpharm.2017.08.087%0Ahttp://dx.doi.org/10.1016/j.ccr.20
879 11.01.031.

880 [52] G.K. Glass, A.C. Roberts, N. Davison, Sacrificial anode and true treatment of concrete,
881 US 2012/0261270 A1, 2012.

882 [53] E.F. Stephan, P.D. Miller, Solubility of Lithium Hydroxide in Water and Vapor Pressure
883 of Solutions above 220° F, J. Chem. Eng. Data. 7 (1962) 501–505.
884 https://doi.org/10.1021/je60015a018.

885 [54] G. Milano, M. Luebben, M. Laurenti, S. Porro, K. Bejtka, S. Bianco, U. Breuer, L.
886 Boarino, I. Valov, C. Ricciardi, Ionic Modulation of Electrical Conductivity of ZnO Due
887 to Ambient Moisture, Adv. Mater. Interfaces. 6 (2019) 1–9.
888 https://doi.org/10.1002/admi.201900803.

889 [55] T.K. Roy, D. Sanyal, D. Bhowmick, A. Chakrabarti, Temperature dependent resistivity
890 study on zinc oxide and the role of defects, Mater. Sci. Semicond. Process. 16 (2013)
891 332–336. https://doi.org/10.1016/j.mssp.2012.09.018.

892 [56] M. Natesan, G. Venkatachari, N. Palaniswamy, Kinetics of atmospheric corrosion of
893 mild steel, zinc, galvanized iron and aluminium at 10 exposure stations in India, Corros.
894 Sci. 48 (2006) 3584–3608. https://doi.org/10.1016/j.corsci.2006.02.006.

895 [57] S.H. Mameno, R. Pettersson, C. Leygraf, L. Wegrelius, Atmospheric corrosion
896 resistance of stainless steel: Results of a field exposure program in the middle-east, Eur.
897 Corros. Congr. EUROCORR 2015. 2 (2015) 1244–1254.
898 https://doi.org/10.1007/s00501-016-0447-9.

899

Manuscript ID: JBE-D-21-02393

Manuscript title: Long-term performance of galvanic anodes for the protection of steel
                   reinforced concrete structures

Highlights

1. Alkali-activated galvanic anodes could protect the reinforcement from corrosion for minimum 12 years
2. Pore size distribution and pH of encapsulating mortar surrounding to galvanic metals were found to significantly affect the performance of galvanic anodes
3. Mechanisms of degradation of alkali-activated galvanic anodes during service are proposed
4. Recommendations to design durable alkali-activated galvanic anodes are proposed

The authors declare that there is no conflict of interest regarding the publication of this article '**Long-term performance of galvanic anodes for the protection of steel reinforced concrete structures**.

Mr. Deepak K. Kamde   **Dr. Radhakrishna G. Pillai**